

AD 726192

ER 7530

# **A COMPARISON OF HYDROGEN EMBRITTLEMENT AND STRESS CORROSION CRACKING IN HIGH STRENGTH STEELS**

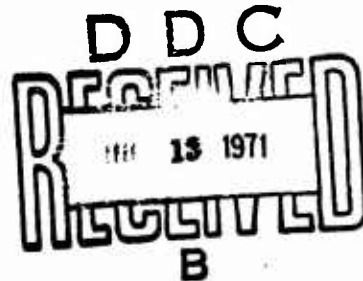
## **TECHNICAL REPORT**

Prepared for  
Office of Naval Research  
Contract N0014-69-C-0286

JUNE 15, 1971

By  
C. S. KORTOVICH  
E. A. STEIGERWALD

Reproduced by  
NATIONAL TECHNICAL  
INFORMATION SERVICE  
Springfield, Va. 22151



**TRW**  
EQUIPMENT GROUP  
MATERIALS TECHNOLOGY

DISTRIBUTION STATEMENT A

Approved for public release;  
Distribution Unlimited

33

**Best  
Available  
Copy**

ER 7530

Technical Report

A COMPARISON OF HYDROGEN EMBRITTLEMENT AND STRESS  
CORROSION CRACKING IN HIGH-STRENGTH STEELS

Prepared for  
Office of Naval Research  
Contract N00014-69-C-0286

June 15, 1971

By  
C. S. Kortovich  
and  
E. A. Steigerwald

TRW Inc.  
TRW Equipment  
Materials Technology  
Cleveland, Ohio 44117

## FOREWORD

The work described in this report was performed under sponsorship of the Office of Naval Research, Contract N00014-69-C-0286 with Dr. P. Clarkin acting as program manager for the Navy. The effort on this contract during the first year dealt with "A Critical Evaluation of Hydrogen Embrittlement Mechanisms" and a paper on this subject was published in Metallurgical Transactions, Vol. 1, December 1970. The second year effort, covered in this report, involved a study of the delayed failure of high-strength steel in aqueous environments. This type of embrittlement has also been attributed to hydrogen generated by the reaction of the metal-environment couple. Attempts were made in this study to relate the mechanisms involved with "classical" hydrogen embrittlement, where the hydrogen is present in the specimen before testing, to the behavior observed in environmentally-induced failure where the hydrogen is continuously generated at the specimen surface.

This report has been assigned TRW Equipment Number ER 7530 and the data are reported in laboratory notebook No. 481.

### ABSTRACT

The purpose of this study was to compare the known behavior of hydrogen embrittled high-strength steel to the characteristics of environmentally-induced stress corrosion failure where hydrogen is continuously generated at the specimen surface. The incubation time for the initiation of slow crack growth was accelerated by prestressing for a fixed time below the lower critical limit. These results obtained on high-strength steel in a stress corrosion environment were directly comparable to behavior of hydrogenated specimens. These data along with hydrogen diffusivity measurements and the insensitivity of the incubation time and crack growth rate to specimen thickness indicated that the stress corrosion process was controlled by the distilled water-metal surface reaction.

## INTRODUCTION

The susceptibility of high-strength steels to delayed failure under sustained load represents a critical performance consideration and an intriguing theoretical problem. The ability of hydrogen to produce delayed failure has been the subject of considerable study, and both the phenomenological and mechanistic aspects of the problem have been well documented<sup>1-4</sup>. Essentially the hydrogen-induced delayed failure problem deals with hydrogen present in the specimen prior to the application of a load. The specimen is usually cadmium plated so that relatively little hydrogen escapes during the test. Thus, a "closed" hydrogen system is involved where the gross hydrogen content remains virtually constant during the test period<sup>2,5,6</sup>. Under these conditions the delayed failure behavior in notched specimens consists of the following characteristics: (1) an incubation time which precedes crack initiation, (2) a period of slow crack growth which is usually discontinuous in nature, and (3) a lower critical stress below which failures are not observed in times of engineering significance.

In cases where cracking does not occur during the introduction of hydrogen into the specimen (irreversible embrittlement) the incubation time is reversible with respect to the applied stress<sup>4,6</sup>, that is, the original incubation time is recovered by removing the stress followed by aging. The incubation time and the recovery process can be directly identified with hydrogen diffusion by activation energy and kinetic considerations<sup>5,6</sup>.

The environmentally-induced delayed failure of high-strength steel in aqueous media has many phenomenological aspects which are similar to failure in hydrogen charged specimens. A typical delayed failure curve for the stress corrosion process, shown in Figure 1, illustrates the presence of an incubation time, a region of slow crack growth and a lower critical limit<sup>7</sup>. Other similarities involve: (1) the activation energy for crack growth in specimens exposed to distilled water which is comparable to that obtained in hydrogenated specimens<sup>5,8,9</sup>, (2) the correlation of hydrogen permeability with environmental cracking<sup>10,11</sup>, and (3) the increase in cracking susceptibility by the inclusion of additions to the environment which are known to facilitate hydrogen absorption<sup>7</sup>. Although the delayed failure of high-strength steel in aqueous media can be attributed to a hydrogen embrittlement mechanism, there are basic differences in the conditions involved in environmental delayed failure and those obtained in specimens charged with hydrogen prior to testing. For example, the charged specimens represent a "closed" hydrogen system and are not dependent on the effectiveness of the external surface reaction to produce hydrogen.

The purpose of this study was to evaluate selected characteristics of the stress corrosion process to allow a direct comparison with reversible hydrogen embrittlement behavior. These results should then provide an indication of whether the classical hydrogen embrittlement results can be used to predict high-strength steel behavior in aqueous environments. The experimental

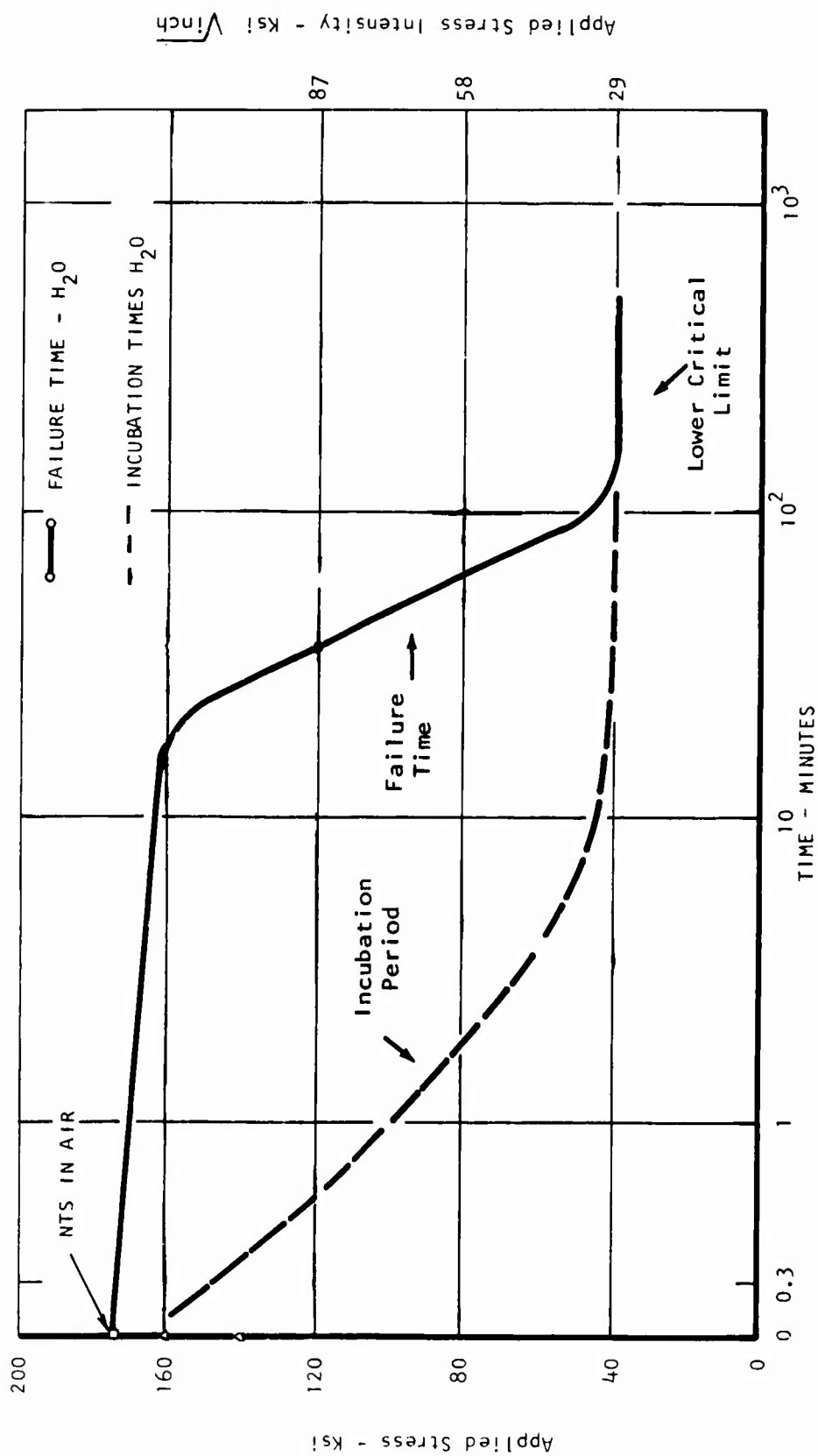


Figure 1. Typical Delayed Failure Curve for AISI 4340 Steel Pre-cracked Sheet Specimens in Distilled Water.

approach involved the evaluation of the conditions in environmentally-induced delayed failure which controlled the incubation time, specifically the reversibility of the incubation time with respect to applied stress, the crack growth behavior, and the lower critical stress. These parameters were studied as a function of material strength level, and specimen thickness, and compared with the known behavior obtained in hydrogen-charged specimens.

#### Materials and Procedure

A commercial heat of 0.067" thick air melted SAE-AISI 4340 steel sheet with the following composition was used for the delayed failure tests.

#### Composition of 4340 Steel (weight percent)

<u>C</u>	<u>Mn</u>	<u>Si</u>	<u>Ni</u>	<u>Cr</u>	<u>Mo</u>	<u>P</u>	<u>S</u>	<u>Fe</u>
0.39	0.85	0.86	1.75	0.87	0.27	0.012	0.22	Balance

The tests were conducted on center-notched precracked specimens having the configuration shown in Figure 2. The specimens were precracked in tension-tension fatigue after heat treatment using a peak stress value less than one-third of the yield strength. The influence of specimen thickness was evaluated using thicknesses of 0.067, 0.040, and 0.020" obtained by grinding the 0.067" specimens to the desired thickness. The specimens were heat treated prior to finish machining according to the following sequence:

1. Normalize 15 minutes, salt bath at 1700°F, air cool.
2. Austenitize 30 minutes, salt bath at 1550°F, oil quench.
3. Temper, 1 hour at 750°F, 700°F, or 400°F, air cool.

The mechanical properties produced by these heat treatments are summarized in Table 1.

Table 1

#### Room Temperature Mechanical Properties of 4340 Steel

	<u>Tempering Temperature, °F</u>		
	<u>750</u>	<u>700</u>	<u>400</u>
Ultimate Tensile Strength (ksi)	197	210	269
0.2% Yield Strength (ksi)	178	189	213
% Elongation (1" G.L.)	8.0	7.5	9.0



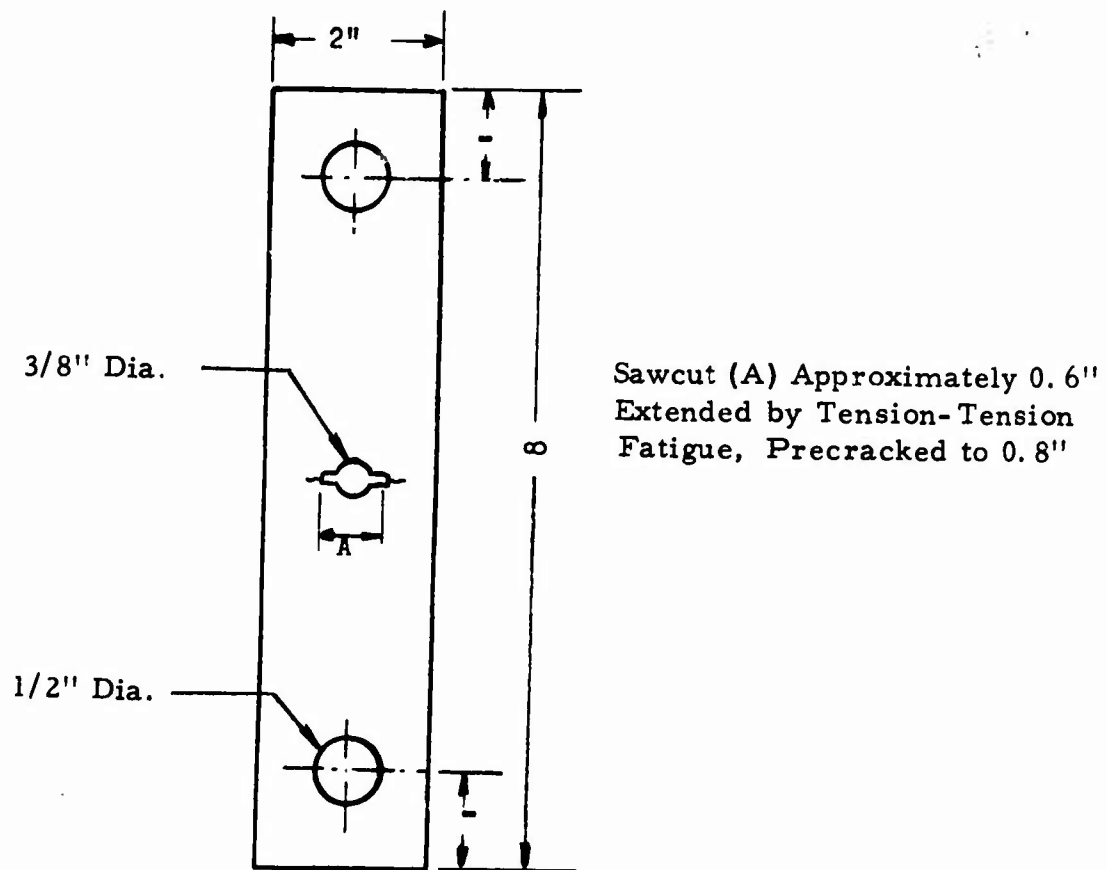


Figure 2. Center Notched, Precracked Tensile Specimen.

The delayed failure tests were conducted on constant load lever arm machines in distilled water. The environment was applied immediately before the application of the load by attaching a plexiglass-neoprene container to the specimen. Crack initiation and growth characteristics of center pre-cracked specimens were measured by recording changes in the specimen compliance using a clip gage beam and a strain bridge output fed to a single pen recorder. A typical crack growth curve obtained from a 4340 precracked specimen exposed to distilled water is shown in Figure 3. The incubation period was defined as the time required for the crack to extend an average of approximately 0.010". The delayed failure data are presented in terms of both the notch tensile stress and applied stress intensity factor (K). The notch tensile stress was defined as the applied load divided by the net specimen area. The stress intensity factor for the center-notch specimens was calculated from the following equation:

$$K = \frac{1.77P\sqrt{a}}{BW} \left[ 1 - 0.1\left(\frac{2a}{W}\right) + \left(\frac{2a}{W}\right)^2 \right]$$

where: K is the applied stress intensity factor,

P is the applied load,

2a is the crack length,

B is the specimen thickness, and

W is the specimen width.

To study the possible influence of surface reactions and hydrogen diffusion on environmentally-induced delayed failure, hydrogen permeability measurements were conducted on the four steels shown in Table 2. The materials were heat treated according to the schedule given in Table 3 and then individually surface ground to a nominal thickness of 0.010". Comparisons were then made between delayed failure properties and hydrogen diffusion. Variations in thickness across any single sample were controlled to within  $\pm 5 \times 10^{-5}$  in. Final preparation of the test foils was by hand finishing with abrasive papers to produce a surface roughness of 15-20 rms. Specimen discs were cut from the foils leaving a tab for electrical contact.

The determination of permeability and diffusion rates was conducted using two independent methods. In one case a modified Sieverts apparatus similar to that previously described<sup>10</sup> was used to measure the hydrogen passing through a membrane into an evacuated known volume. One side of the membrane was exposed to a 3.0N NaCl solution, and the membrane was at a -1240 mv potential with respect to a saturated calomel electrode. The permeability was determined from the pressure rise as a function of time, while the comparative diffusivities were determined from the time lag<sup>12</sup>.

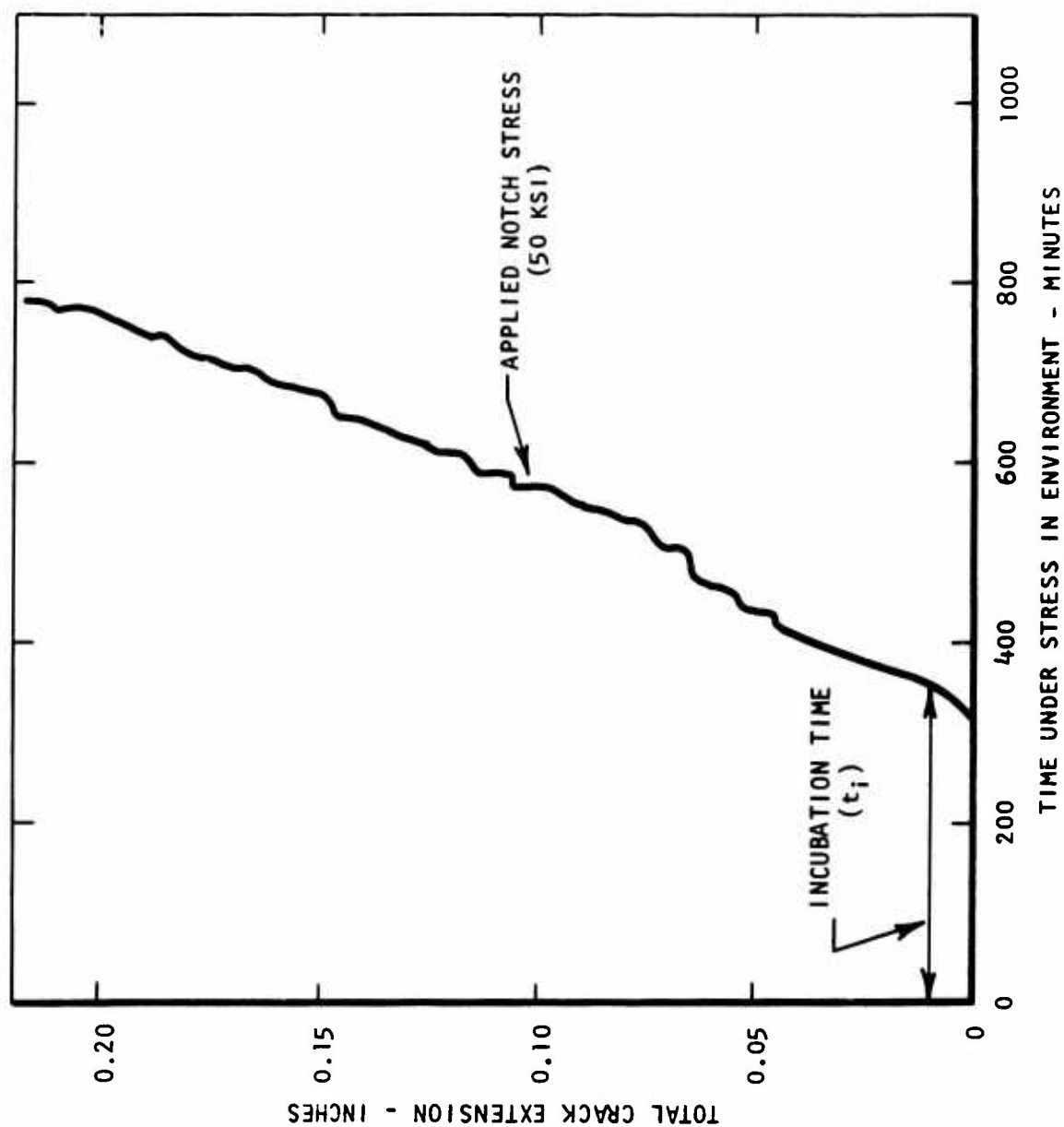


Figure 3. Typical Crack Growth Curve Obtained From Precracked 4340 Steel Specimen 0.067" Thick, 750°F Temper, Distilled Water Environment.

Table II

## Composition of High-Strength Steels Used in Permeability Studies

Alloy	Source and Heat No.	C	Si	Mn	Cr	V	Mo	Co	Ni	P	S
D6AC	Vanadium-Alloys CVM 3960529	0.48	0.21	0.73	1.08	0.08	1.02		0.63	0.009	0.007
4340	Republic CVM 3951969	0.40	0.25	0.72	0.81		0.27		1.81	0.007	0.005
H-11	Vanadium-Alloys VASC0 03132	0.40	0.88	0.26	4.88	0.53	1.29			0.008	0.007
HP 9-4-45	Republic CVM 3921091	0.43	0.01	0.15	0.32	0.09	0.30	3.95	7.80	0.006	0.009

Table III

## Heat Treatments and Properties of High-Strength Steels Used in Permeability Studies

Steel	Heat Treatment	U.T.S. ksi	0.2% Y.S. ksi
AISI 4340	Normalize at 1700°F for 15 minutes in salt, air cool. Austenitize at 1550°F, oil quench. Temper at 600°F 1 + 1 hour.	240.1	206.6
D6AC	Austenitize at 1500°F $\pm 25^\circ\text{F}$ for 20 minutes in salt, oil quench. Temper at 850°F for 1 hour plus 850°F for 1 hour.	234.7	224.8
HP 9-4-45	Normalize at 1600°F, 30 minutes in salt, air cool. Austenitize at 1450°F, 15 minutes in salt, oil quench. Temper at 650°F, 2-1/4 hours.	239.8	224.4
H-11	Preheat to 1325°F $\pm 25^\circ\text{F}$ in salt. Austenitize at 1850°F $\pm 15^\circ\text{F}$ for 30 minutes in salt, air cool. Temper in 1060°F 2 + 2 hours.	243.5	205.6

A separate measure of diffusivity was obtained at the University of Pennsylvania using their electrochemical permeation technique<sup>13</sup>. In this method the specimen was cathodically charged with hydrogen from one side with the hydrogen diffusing through being oxidized by maintaining a sufficiently anodic potential. The rate at which hydrogen diffuses through the membrane is determined by the current needed to maintain the constant anodic potential at this surface. The permeation current is recorded as a function of time starting with the initiation of charging. Such experimental permeation transients were then compared with the theoretically predicted curve to calculate the diffusion coefficients. Although the experimental build-up transients had the expected shape, they did not fit the theoretical curve (based on a constant  $D$ ) exactly. By fitting the experimental curves to the theoretical at short time, intermediate time and long time, three  $D$  values were calculated. A number of replicate permeation runs were made with each sample and the average  $D$  values were determined.

In the electrochemical permeation technique, the steel samples were initially polished with emery papers (0/0 to 4/0), washed with soap and water, cleaned with a 1% HCl solution in methanol, washed in distilled water, benzene, methanol and then acetone. The anodic side of the specimen was coated with palladium to prevent excessive corrosion during the permeation. All permeations were made using 0.2N NaOH solution which was pre-electrolyzed using platinum electrodes.

## RESULTS AND DISCUSSION

The comparison of stress corrosion failure in high-strength steels with hydrogen embrittlement predictions will be made in terms of three parameters: the incubation time, the crack growth kinetics, and the lower critical stress. The main emphasis will not involve reaffirming that environmental failure is associated with hydrogen<sup>7,10,11</sup> but rather to determine whether the presence of the externally generated hydrogen is rate controlling. When this condition occurs, a direct translation of the hydrogen embrittlement results obtained in specimens containing hydrogen may not be possible, and an understanding of the causes for the differences could aid in minimizing the high-strength steel delayed failure problem in aqueous environments.

### Incubation Time Effects

The incubation time required for the initiation of slow crack growth in a hydrogenated high-strength steel specimen has been identified as the time required for a critical quantity of hydrogen to diffuse to a region of maximum triaxiality<sup>2</sup>. Removal of the stress prior to cracking causes a recovery of the incubation time, so that the initiation period is completely reversible with respect to the applied stress<sup>4,6</sup>. Tests were conducted on precracked specimens exposed to distilled water to determine if the incubation time for the initiation of slow crack growth determined under this condition exhibits behavior comparable to hydrogenated sharply-notched specimens. The delayed failure curve for 4340 steel, heat treated to 197 ksi tensile strength is shown in Figure 4. In the test sequence shown by the dashed line in Figure 4 samples were prestressed for 25 hours at a notch tensile stress of 30 ksi which is below the lower critical limit. No crack growth was observed in that period. The load on the specimens was then increased to a level within the delayed failure region and the incubation time was compared to that observed on specimens which were not prestressed. The results shown in Figure 5 indicate that a significant decrease in incubation time occurred as a result of prestressing below the lower critical limit. This behavior can be attributed to either hydrogen diffusion into the specimen during the prestressing period<sup>14</sup> or to dissolution of a protective film or oxygen barrier<sup>15</sup> which would allow the hydrogen producing surface reaction to be initiated in less time.

To more completely examine which mechanism was operative, specimens prestressed below the lower critical limit were held at various times at room temperature without stress to determine the recovery kinetics of the incubation process. The results of these tests are shown in Figure 6. When the specimens prestressed below the lower critical limit were allowed to age in air without a load the incubation time returned to its initial value in approximately 100 hours. The implication of these experiments is either: (1) the hydrogen grouping produced by the application of stress below the lower critical limit was eliminated by the removal of the stress, or (2) the barrier film was reformed by exposure to air. The rate of recovery was

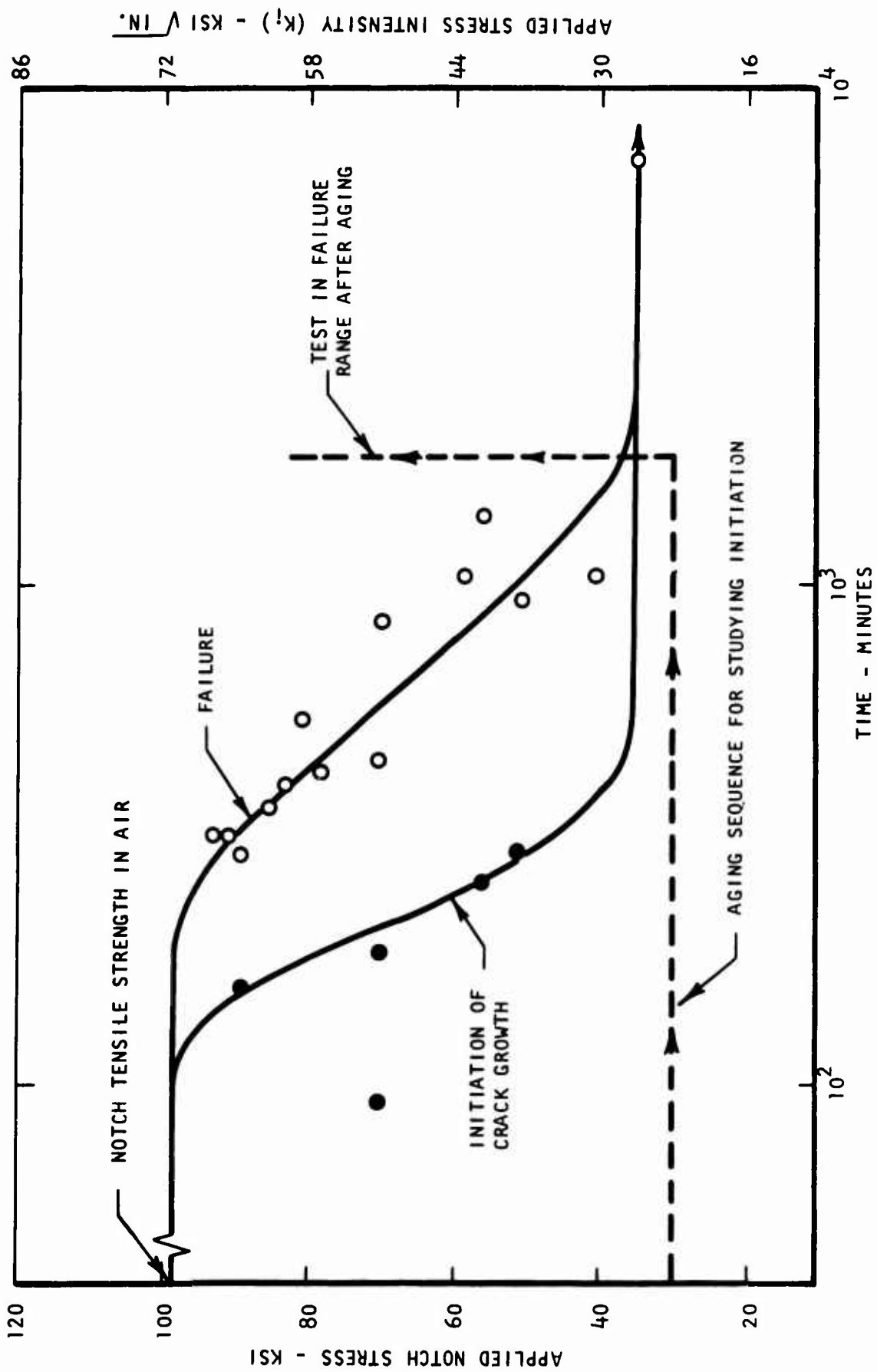


Figure 4. Delayed Failure Curve for 4340 Steel, 750°F Temper, Exposed to Distilled Water Environment, Pre-cracked Specimens, 0.067" Thick.

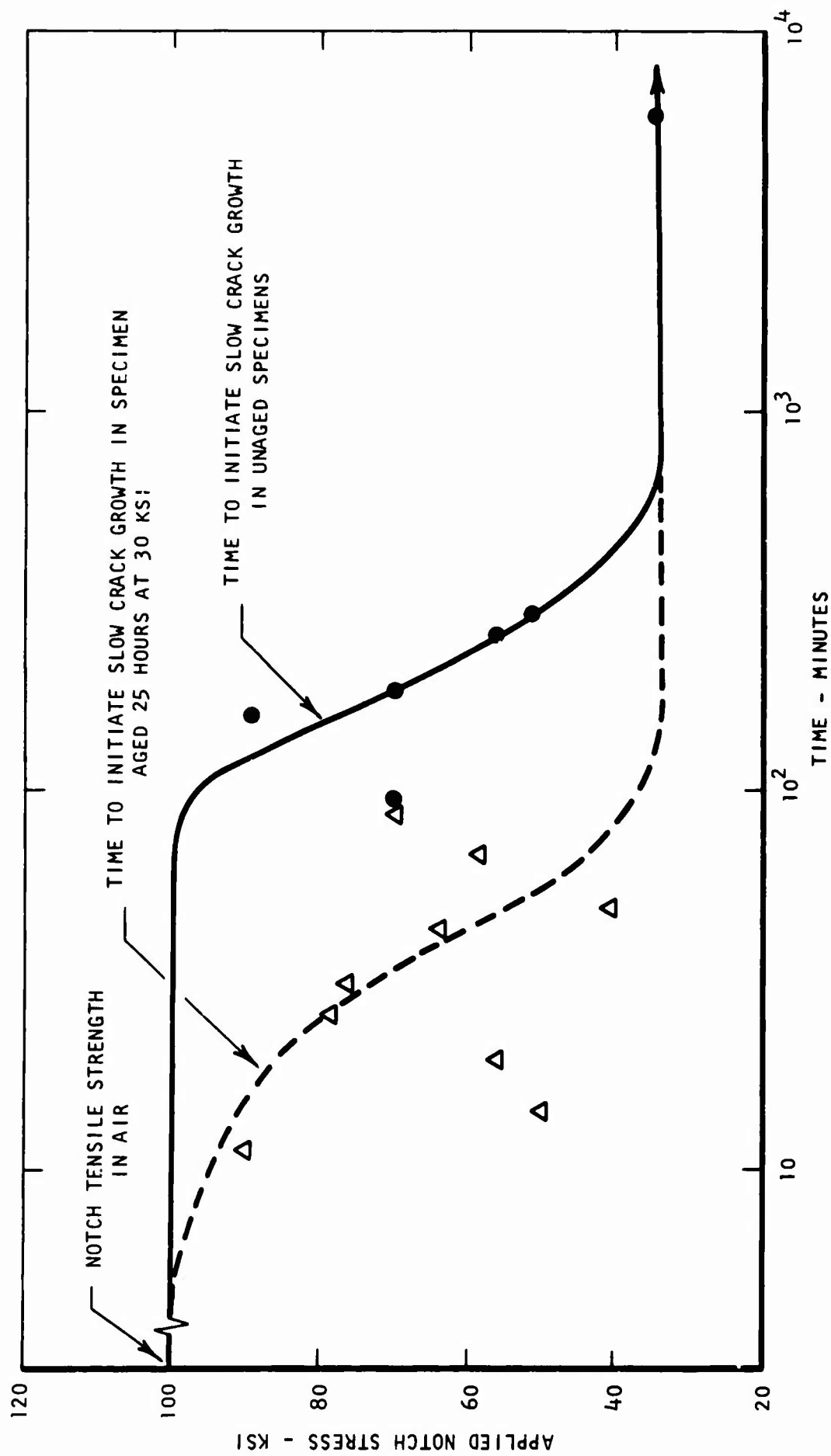


Figure 5. Influence of Aging Below the Lower Critical Limit on the Time to Initiate Slow Crack Growth, 4340 Steel 750°F Temper, Pre-cracked Specimens, 0.067" Thick.



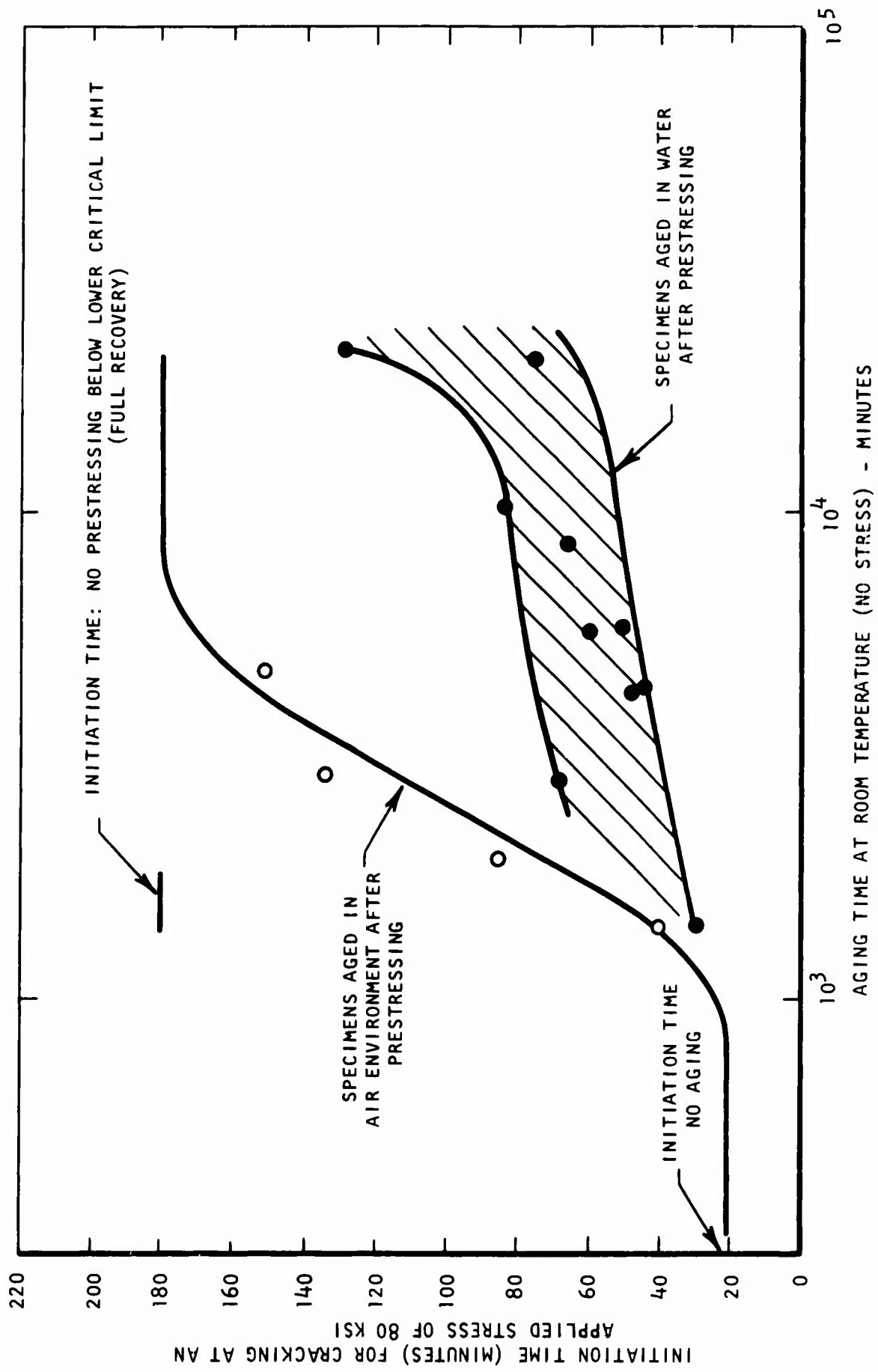


Figure 6. Recovery Curve for Incubation Time After Prestressing Below the Lower Critical Limit, 4340 Steel, 750°F Temper, 0.067" Thick.

examined with a second group of specimens which were aged in water, rather than air. In this case, also shown in Figure 6, the incubation time was not completely recovered even after exposures as long as 360 hours. The results indicate that in the times involved in the experiments the incubation time was completely reversible only when an air environment was used and that complete reversibility with respect to applied stress is significantly slower in an aging environment of water. On this basis the incubation time in the failure of high-strength steel precracked specimens exposed to aqueous environments can best be defined as the time required for the environment to penetrate some type of protective film which forms at the crack tip during or subsequent to the fatigue precracking operation. When aging occurs in an air environment, the film reforms and the incubation time is recovered; when aging occurs in water, the ability to reform the film is altered, and total recovery is retarded.

An analysis of the kinetics of the recovery process also provides some additional support to the presence of a barrier as the critical element controlling incubation time. The recovery time for the incubation period in hydrogenated sharply-notched specimens is an order of magnitude faster than recovery in precracked specimens exposed to distilled water<sup>6</sup>. The kinetics observed in these stress corrosion studies are not consistent with the diffusion model used to explain recovery in hydrogen-charged specimens.

If the incubation time for the initiation of crack growth in environmentally-induced failure of high-strength steel represents the time required for the environment to penetrate a barrier and reach the crack tip so that it can start reacting to form hydrogen, then this time should be relatively independent of specimen thickness. The results obtained on tests conducted with 0.020" and 0.040" thick 4340 specimens exposed to a distilled water environment are shown in Figures 7 and 8, while the data for the 0.067" thick specimens were presented in Figure 4. The incubation time for the onset of stable crack growth was comparable under these conditions and not a function of specimen thickness. In the case of 0.067" thick specimens heat treated to a variety of strength levels, the incubation time did, however, show a significant dependence on the heat treatment (see Figures 9 and 10). The specimens tempered at 400°F had essentially no incubation period. This could be attributed to an extension of the crack during the application of the static load. As a result a fresh crack surface was immediately exposed to the environment and no barrier permeation was necessary. A photograph of the degree of crack extension produced by applying the static load and heat tinting is shown in Figure 11A. The 700°F tempered specimens exhibited slight tearing at isolated points along the crack front (Figure 11B) while no measurable crack extension occurred in the specimens tempered at 750°F (Figure 11C). The incubation time was then inversely related to the fresh crack surface that was exposed during the application of the initial load. A description of the incubation period as the time required for the environment to permeate a barrier and react with the crack tip is then consistent with these experimental data.

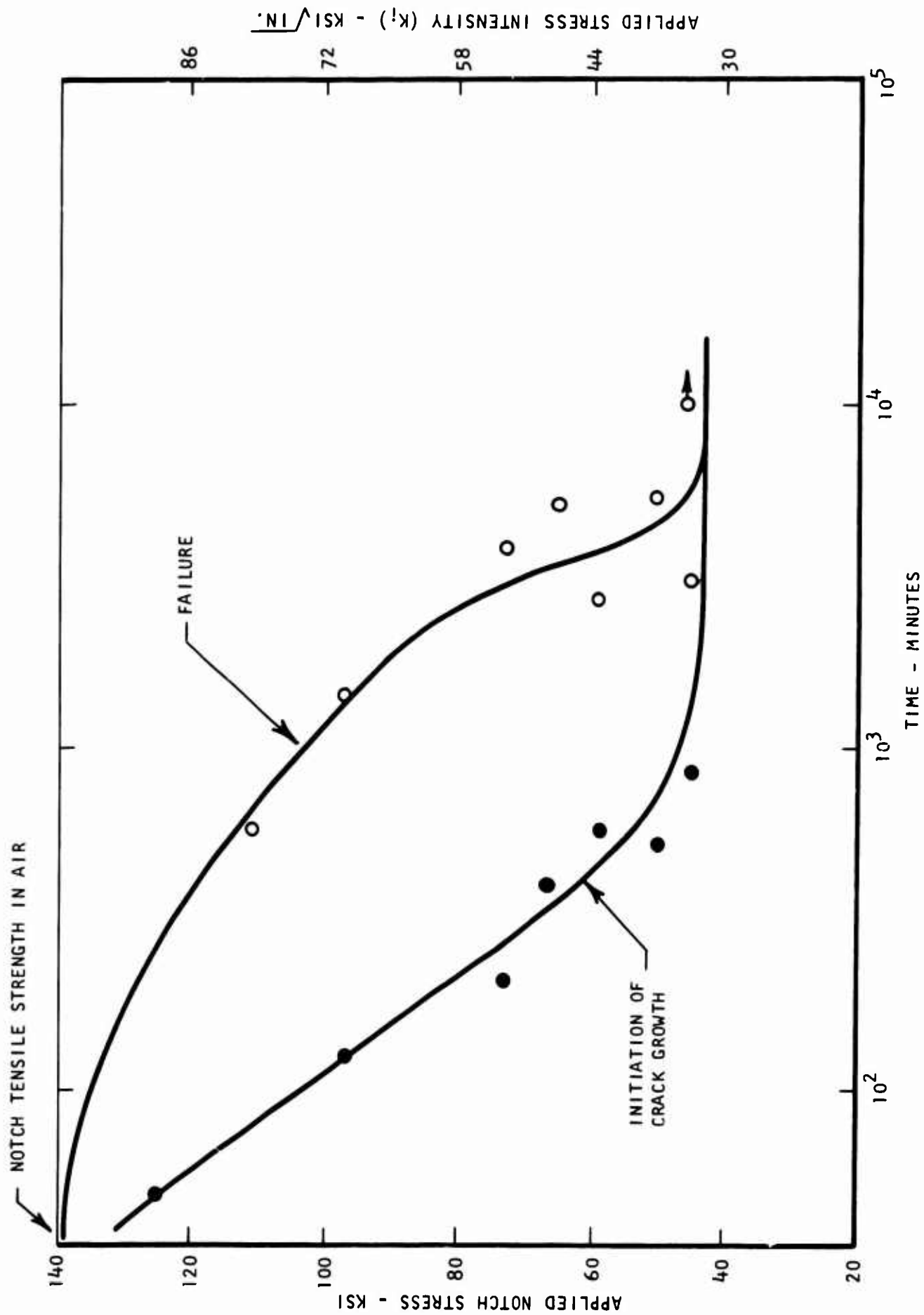


Figure 7. Delayed Failure Curve for 4340 Steel, 750°F Temper, Exposed to Distilled Water Environment, Precracked Specimens, 0.020" Thick.

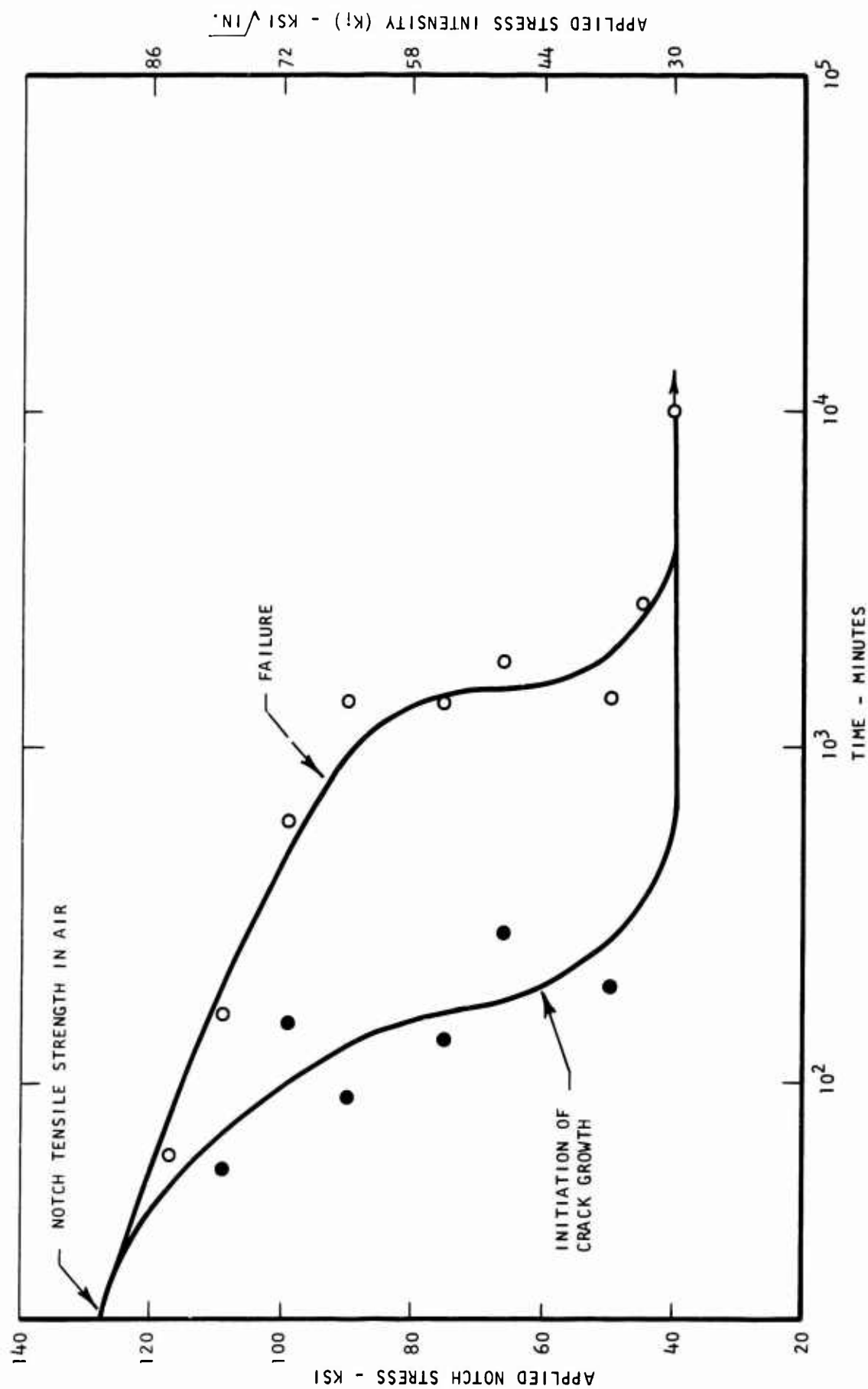


Figure 8. Delayed Failure Curve for 4340 Steel, 750°F Temper, Exposed to Distilled Water Environment, Pre-cracked Specimen, 0.040" Thick.

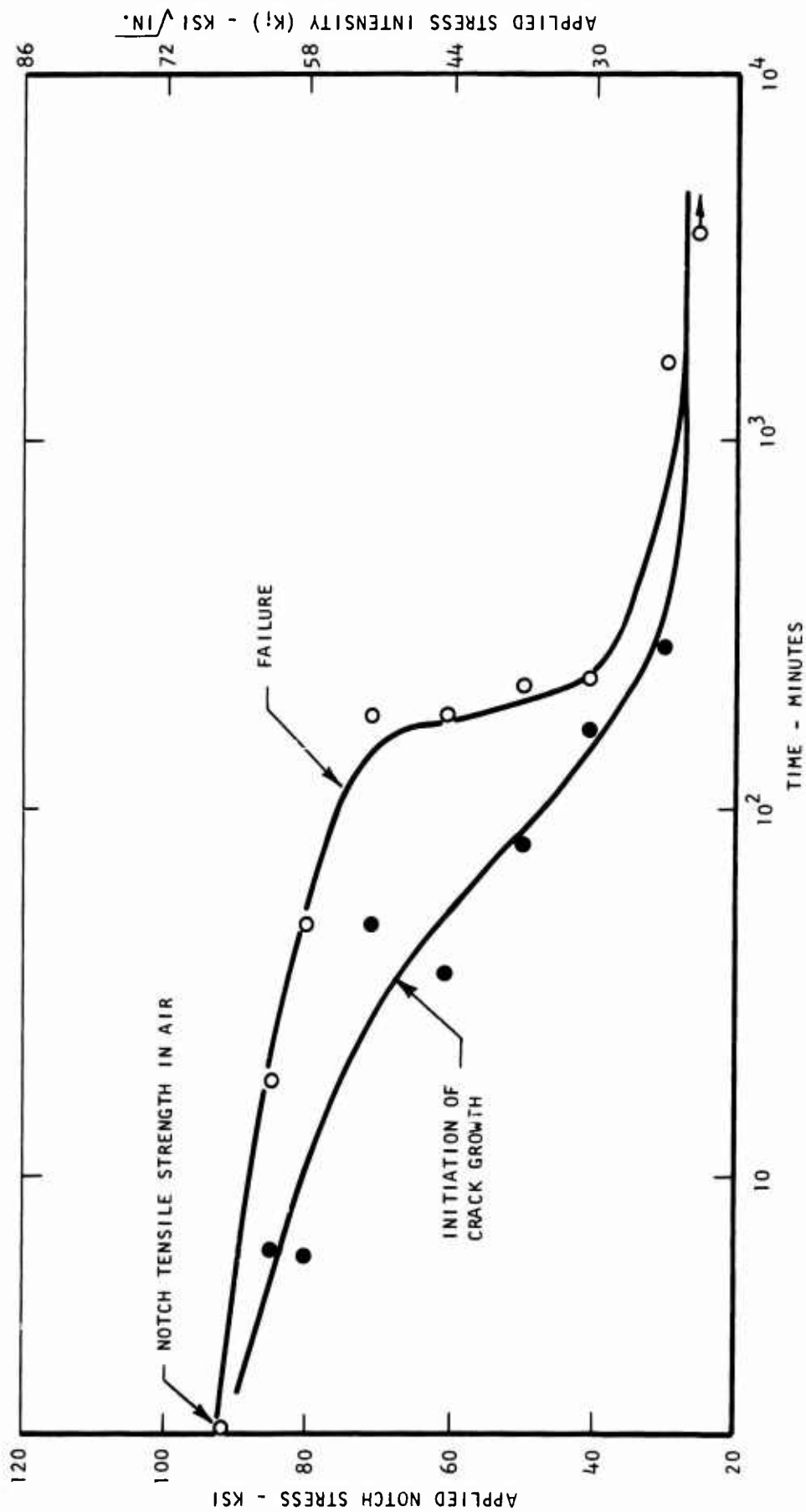


Figure 9. Delayed Failure Curve for 4340 Steel, 700°F Temper, Exposed to Distilled Water Environment, Pre-cracked Specimens, 0.067" Thick.

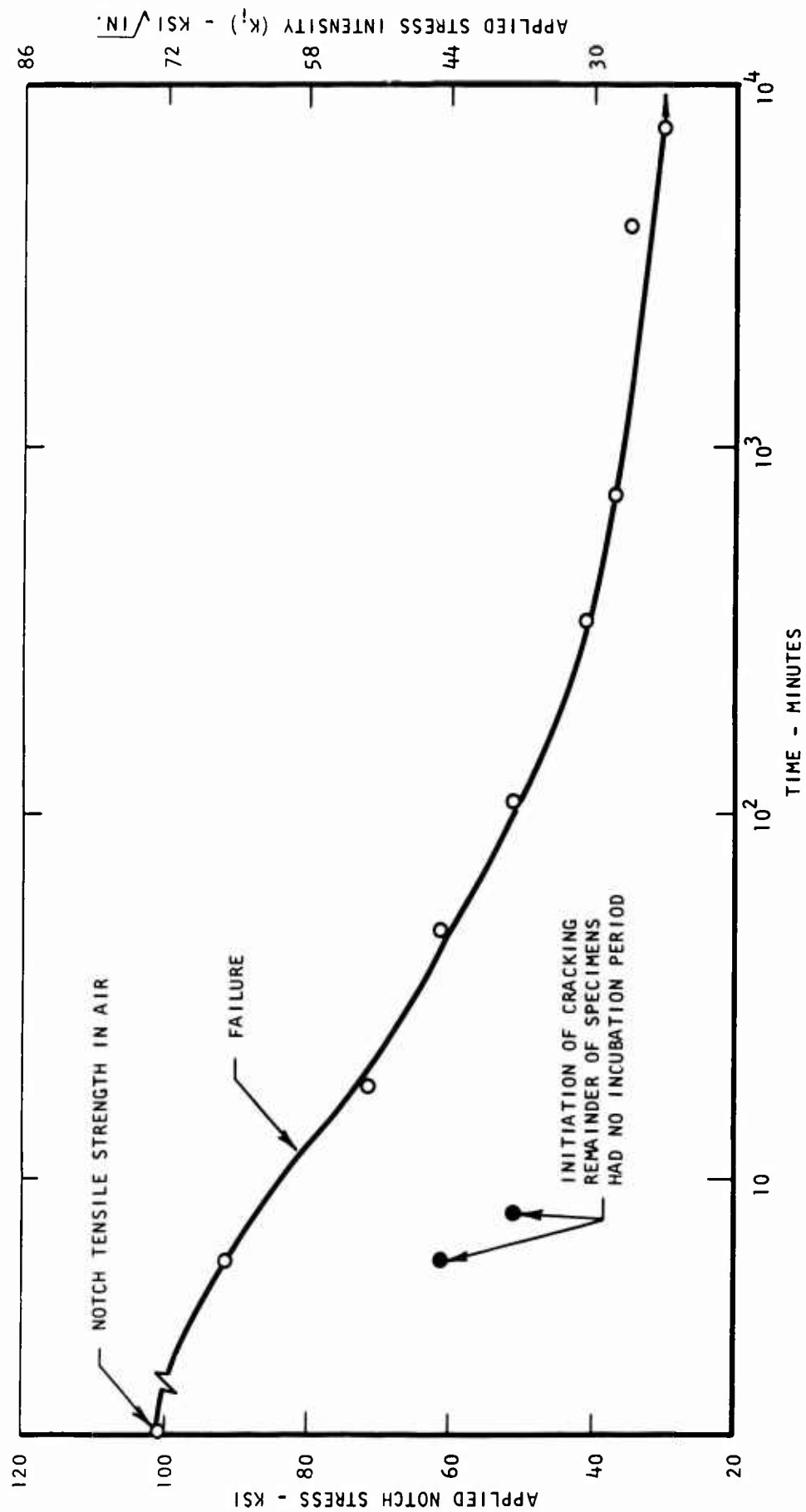


Figure 10. Delayed Failure Curve for 4340 Steel, 400°F Temper, Exposed to Distilled Water Environment, Precracked Specimens, 0.067" Thick.

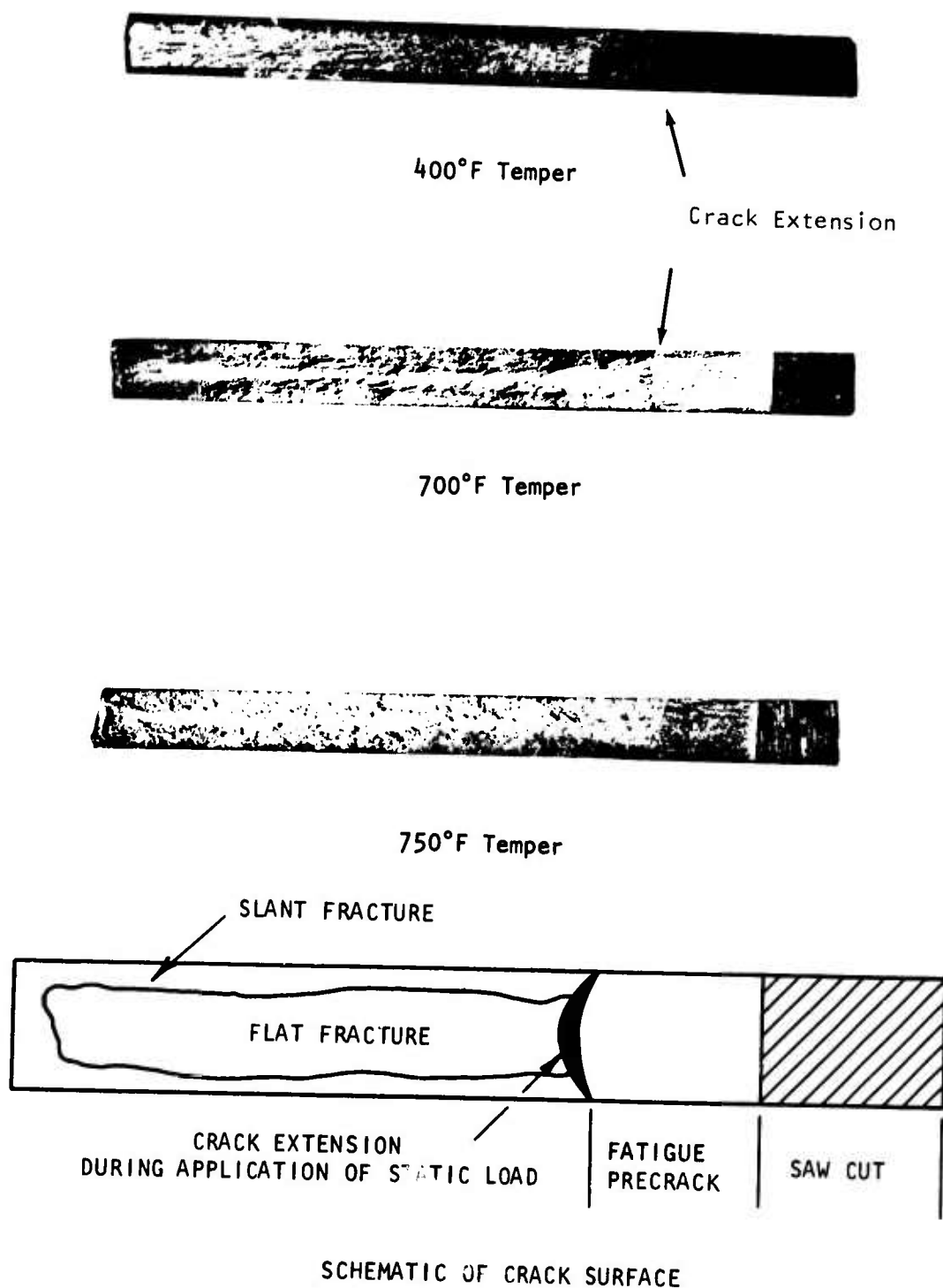


Figure 11. Schematic and Actual Crack Surfaces of 0.067" Thick Specimens Tested in Air Environment. Specimens Loaded to 60 ksi, Unloaded, Heat Treated 1 Hour at 600°F, and Reloaded to Failure.

### Crack Growth Behavior

Once the crack started, the prior aging or recovery conditions used in the tests to study incubation time had no significant effect on the crack growth kinetics. Both specimen thickness and heat treatment did, however, have a significant influence on the failure time. To determine the cause for these differences, consideration must be given to the basic toughness of the material as well as the crack growth kinetics. For example, a longer failure time could occur, not because the material has a greater resistance to stress corrosion failure, but because the crack simply had to grow a longer distance before the critical crack length, hence total specimen failure, occurred. Thinner specimens have a greater inherent fracture toughness due to the reduced constraint at the crack tip hence they should exhibit a greater failure time solely on the basis of this consideration. The average crack growth rates for specimens of various thicknesses are compared in Figure 12. The results show that the average crack growth rates for the 4340 steel, tempered at 750°F were essentially independent of specimen thickness. The longer failure times in the specimens with varying thickness were then simply a result of the fact that the crack had to grow a longer distance before failure took place.

In the case of the material heat treated to various strength levels, a definite difference in crack growth behavior was observed. As shown in Figure 13, the steel tempered at the lower temperatures (higher strength levels) had significantly higher average crack growth rates. The exact reason for this difference has not as yet been defined. However, it appears to be related to two factors: (1) the basic susceptibility of the material to hydrogen (generated by the environment), i.e., higher strength steels required less hydrogen for a given degree of embrittlement, and (2) the toughness of the steel which regulates the incremental extension of the crack on a microscale. At present the relative importance of each of these factors has not been defined.

Chemical composition of the steel has also been shown to produce large variations in stress corrosion crack growth rates in addition to strength level<sup>15</sup>. Previously reported variations in crack growth rates for 4340, D6AC, HP 9-4-45, and H-11 heat treated in the 240 ksi tensile strength range are shown in Figure 14. If the crack growth rates are uniquely controlled by hydrogen diffusion from the surface to a critical region below the crack tip then a correlation should exist between the hydrogen diffusivity and the crack growth kinetics. The relationship between the hydrogen diffusivity measured by either the electrolytic permeation method or the pressure increase method are plotted in Figure 15 as a function of average crack growth rates. Although differences in diffusivity existed as a function of measuring technique the general behavior was consistent. No significant variation in diffusivity was apparent for the 4340, D6AC, and HP 9-4-45 over a range of crack growth rates of approximately three orders of magnitude. The H-11 steel was the only material which showed both a decrease in hydrogen diffusivity and a decrease in the rate of crack growth. On the basis of these data it appears



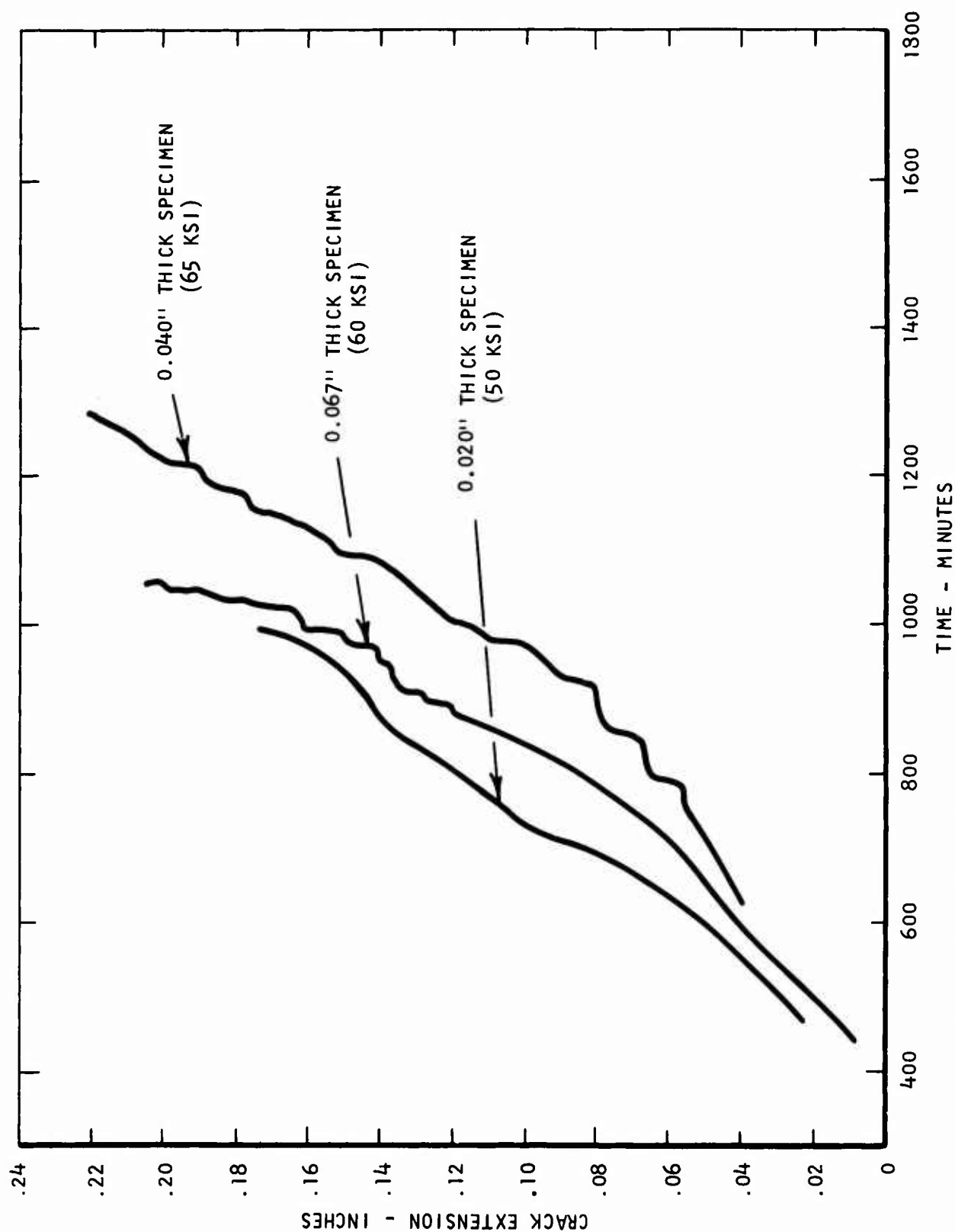


Figure 12. Comparative Crack Growth Curves for 4340 Precracked Specimens of Varying Thickness, 750°F Temper, Distilled Water Environment.

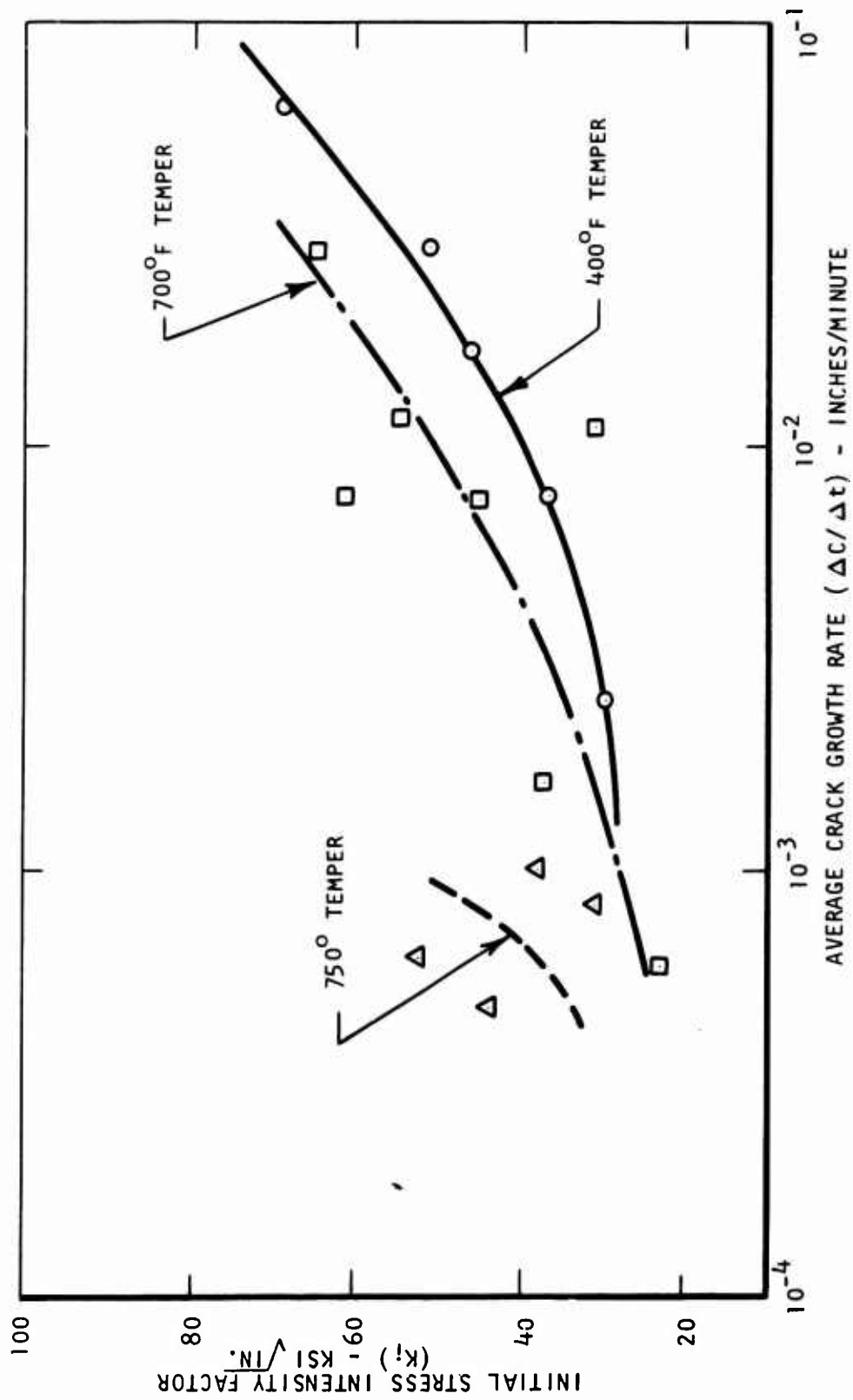


Figure 13. Variation of Crack Growth Rate, 4340 Steel, Distilled Water Environment, Pre-cracked Specimens, 0.067" Thick.

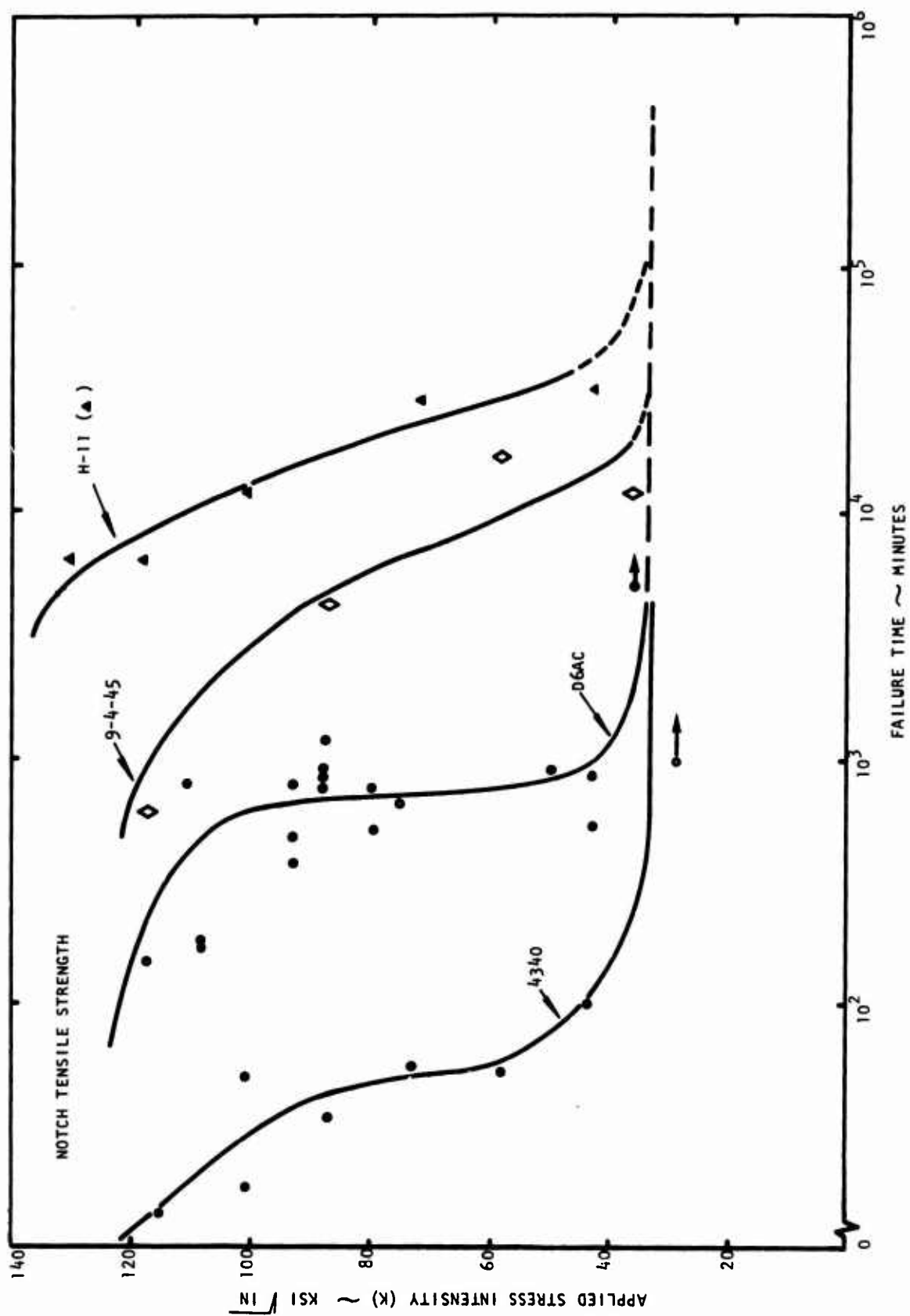


Figure 14. Delayed Failure of High-Strength Steels of Various Compositions in a Distilled Water Environment (from Ref. 15).

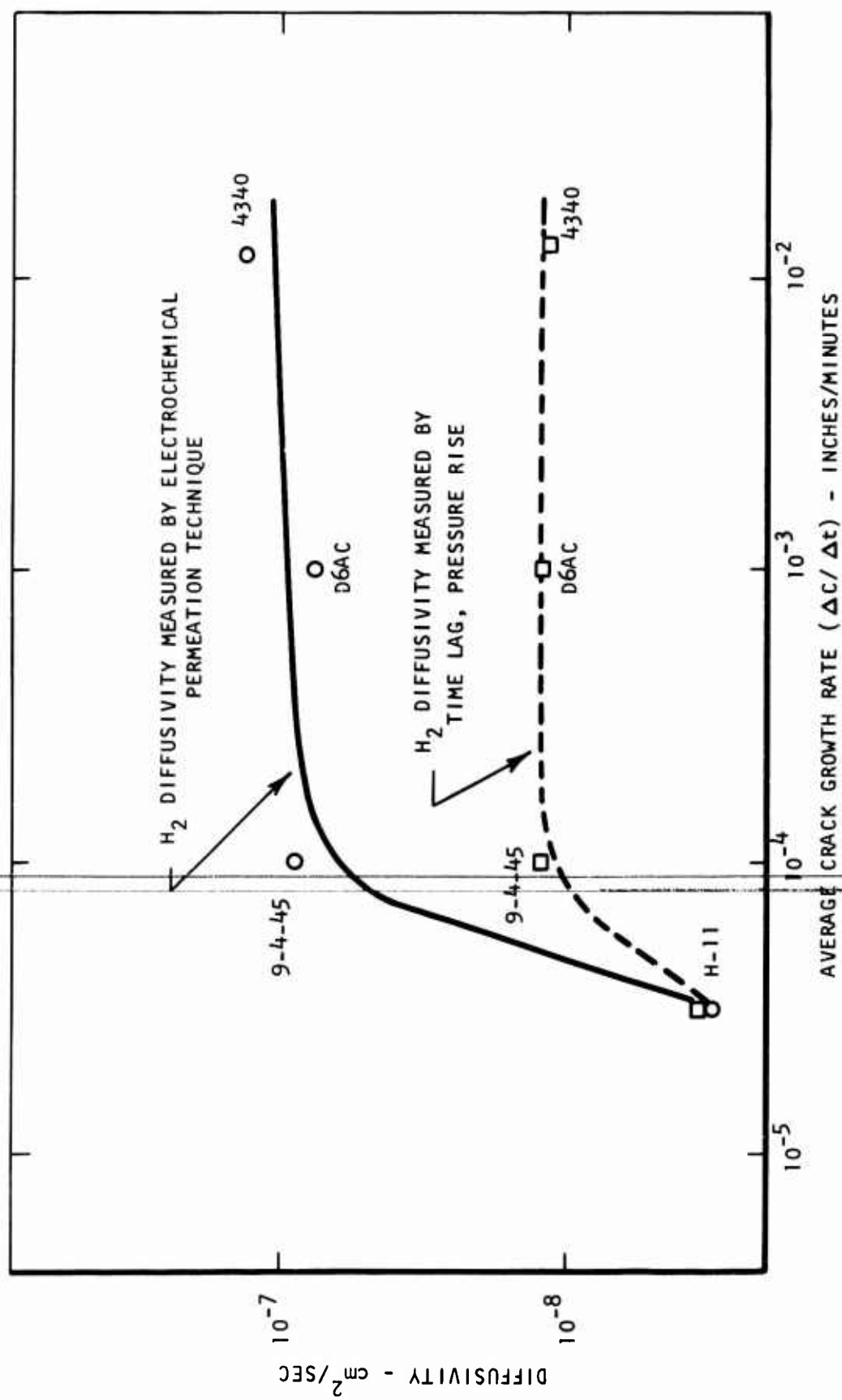


Figure 15. Relationship Between Diffusivity of Hydrogen Through High-Strength Steels and Average Crack Growth Rate of Pre-cracked Specimens Exposed to a Distilled Water Environment.

that hydrogen diffusivity is not rate controlling in the stress corrosion of precracked high-strength steel specimens of 4340, D6AC, and 9-4-45 types as is the case for hydrogenated sharply-notched specimens of 4340. Actually, hydrogen embrittlement predictions indicate that the critical region is the area of maximum triaxiality, and in precracked specimens this would be very close to the crack tip. As the notch acuity is decreased, the triaxial region moves farther from the surface, and under these conditions diffusivity may become controlling. The diffusivity results indicate that the crack growth rate in stress corrosion of precracked steel specimens is governed not by the kinetics of hydrogen movement but by either the rate of hydrogen generation at the surface or the susceptibility of the particular steel to the basic hydrogen embrittlement effect.

#### Lower Critical Limit

Compared to the order of magnitude changes in incubation time and crack growth rates that occur in stress corrosion of high-strength steel as a function of strength level or composition, the changes in lower critical limit are relatively small. If the lower critical limit is considered as the stress below which no failure will occur, then rate effects do not become a consideration. For example, if the failure mechanism depends on the development of a critical hydrogen concentration at the surface or at a slight distance below the surface, then in the region where failure is observed the following prevails:  $C_H > C_{CH}$  where  $C_H$  is the concentration of hydrogen at a specific point and  $C_{CH}$  is the critical hydrogen concentration necessary to produce embrittlement. Below the lower critical  $C_H < C_{CH}$  and no failure would take place. At the lower critical limit, therefore  $C_H = C_{CH}$ . Using Boltzmann statistics to describe the concentration in a manner similar to that performed for hydrogen embrittlement in sharply notched specimens<sup>2,14</sup> or that presented by Liu<sup>16</sup> for stress corrosion leads to the general relation:

$$C_H = C_O e^{-U/kT}$$

where  $C_H$  is the concentration of the critical specie,

$C_O$  is the average concentration,

$U$  is an interaction energy term,

$k$  is the Boltzmann constant, and

$T$  is the absolute temperature.

At the lower critical stress:

$$C_H = C_{CH} = C_O e^{-U/kT}$$

Assuming that for specimens of the same strength level but of varying thickness the  $C_{CH}$  value necessary for embrittlement is a constant, then the lower critical limit is defined by:

$$\ln[C_H/C_O] = \text{constant} = U/kT, \text{ and at a given test temperature}$$

$$U = \text{constant}$$

In cases where stress-induced movement is involved, the interaction energy (U) can be expressed approximately in terms of the applied stress ( $\sigma_{app}$ ) times some appropriate stress concentration factor ( $\alpha$ ):

$$U = \sigma_{app} \alpha = \text{constant}$$

An alternate view is to consider that the concentration of hydrogen does not vary, and a specific stress represented by the lower critical stress is required to produce crack extension. On this basis, the effective stress at the crack tip is above a critical value in the failure range and less than the critical value below the lower critical limit. This reasoning leads to exactly the same conclusion, i.e., the lower critical limit can be defined by the equation

$$\sigma_{app} \alpha = \text{constant}$$

As the thickness is decreased, the effective stress concentration factor  $\alpha$  is decreased because less constraint is present, hence the applied stress (lower critical limit) must be increased to maintain the constant  $\sigma_{app} \alpha$  product. Correspondingly when the strength level is increased, the stresses at the crack tip are not reduced to as large an extent by plastic flow, the  $\alpha$  term is increased and the lower critical limit ( $\sigma_{app}$ ) is reduced.

In an effort to obtain an indication of whether the general behavior trend predicted by the  $\sigma_{app} \alpha = \text{constant}$  relationship applies the lower critical stress was plotted as a function of the ratio of the notch tensile strength to the yield strength squared ( $\sigma_{NTS}/\sigma_{YS}^2$ ). This ratio was considered a qualitative measure of the relative material toughness which should be inversely related to  $\alpha$ . Increasing the ratio should produce an increase in the ability of the material to resist stress build-up at the crack tip, therefore, an increase in the lower critical limit. The results plotted in Figure 16 indicate a generally good agreement with predictions for data obtained on 4340 steel tested at either varying thicknesses or varying strength levels. A more detailed analysis of the results is not warranted because of the qualitative nature of the methods for expressing  $\alpha$ .

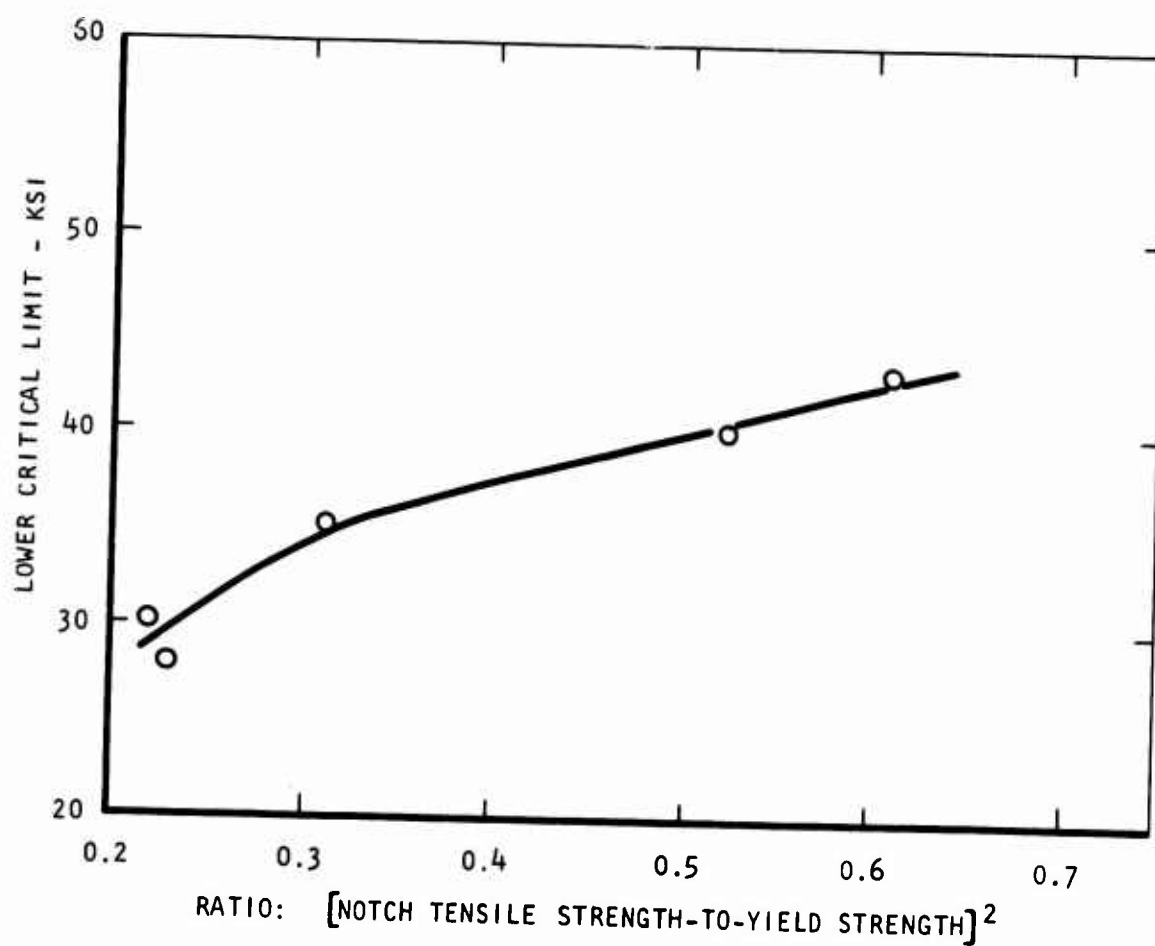


Figure 16. Variation in Lower Critical Limit with Arbitrarily Selected Measure of Relative Material Toughness.

## SUMMARY AND CONCLUSIONS

Experiments were conducted to study the behavior of high-strength steel precracked specimens exposed under static load to a distilled water environment. Although hydrogen embrittlement is regarded as the primary cause for this type of stress corrosion failure, certain differences are anticipated in the characteristics of the failure process in specimens containing hydrogen and those where hydrogen is liberated by a surface reaction. The purpose of this program was to evaluate these differences with respect to the incubation time for the initiation of crack growth, the crack growth rate, and the lower critical limit.

Prestressing for a given time period below the lower critical limit produced a significant decrease in the time required to initiate slow crack growth. Aging studies after prestressing were conducted to examine the reversibility behavior of the incubation time. When the aging was performed in air the incubation time was fully recovered in about 100 hours. Full recovery of the incubation time was not obtained, however where the aging was performed in water even after 360 hours. The results indicated that the incubation time was related to a critical amount of dissolution or permeation of a barrier film at the crack tip. Aging in air allowed the barrier to reform and produced full recovery of the incubation time. Aging in water however retarded the barrier formation and prolonged the recovery process. The results differ from those obtained in hydrogenated specimens where the incubation time was completely reversible with respect to applied stress and the process kinetics could be related to hydrogen diffusion.

The incubation time for the initiation of crack growth was relatively insensitive to specimen thickness but a definite function of material heat treatment. Increasing the strength level of steel by reducing the tempering temperature produced a decrease in crack growth initiation time.

~~The average crack growth rate was not influenced significantly by~~ specimen thickness. The results indicated that the increased failure time present in thinner specimens of 4340 steel resulted from the crack having to grow a greater distance rather than a change in the basic stress corrosion behavior.

The hydrogen diffusivity for high-strength steels of several different compositions was compared to the average crack growth rates. No correlation between crack growth rate and diffusivity was apparent over the range of conditions evaluated. Consistent with the incubation time studies, the diffusivity measurements suggest that the failure process is controlled by the hydrogen generating environment-metal reaction.



The lower critical limit is not as sensitive to heat treatment as the incubation times or crack growth rates. Variations in tensile strength from 289 ksi (400°F temper) to 198 ksi (750°F temper) produced only a 12 ksi difference in lower critical limit. The results could be qualitatively explained on the basis that the applied stress times a concentration factor remains a constant. Decreasing the effective stress concentration factor by raising the strength level or increasing the thickness increased the effective stress at the crack tip and therefore reduced the measured lower critical limit.

## REFERENCES

1. R. P. Frohberg, W. J. Barnett, and A. R. Troiano: Trans. ASM, 1955, Vol. 47, p. 892.
2. A. R. Troiano: Trans. ASM, 1960, Vol. 52, p. 54.
3. N. J. Petch and P. Stables: Nature, Vol. 169, 1952, p. 842.
4. H. H. Johnson, J. G. Morlet, and A. R. Troiano: AIME Trans., Vol. 179, 1957, p. 777.
5. E. A. Steigerwald, F. W. Schaller, and A. R. Troiano: AIME Trans., Vol. 215, 1959, p. 1048.
6. C. F. Barth and E. A. Steigerwald: Met. Trans., Vol. 1, 1970, p. 3451.
7. G. L. Hanna, A. R. Troiano, and E. A. Steigerwald: Trans. ASM, Vol. 57, 1964, p. 658.
8. W. Beck, J. Bockris, J. McBreen and J. Nanis, Proc. Roy. Soc. (London), Vol. A290, 1966, p. 221.
9. H. H. Johnson and A. M. Willner, App. Mat. Res., Vol. 4, 1965, p. 34.
10. C. F. Barth, E. A. Steigerwald, and A. R. Troiano: Corrosion, Vol. 25, No. 9, 1969, p. 353.
11. B. F. Brown, C. T. Fujii, and E. P. Dahlberg: Journal Electrochem. Soc., Vol. 116, 1969, p. 218.
12. ~~R. M. Barrer: Trans. Faraday Soc., Vol. 36, 1940, p. 1235.~~
13. L. Nanis: University of Penn. Tech. Report UPH2-002, December 1970, ONR Contract NR 036-077.
14. E. A. Steigerwald, F. W. Schaller, and A. R. Troiano: Trans. AIME, Vol. 218, October 1960, p. 832.
15. W. D. Benjamin and E. A. Steigerwald: ASM Trans., Vol. 60, No. 3, 1967, p. 547.
16. H. W. Liu: ASME Journal of Basic Eng., September 1970, p. 633.